

Electron trapping and impurity segregation without defects: *Ab initio* study of perfectly rebonded grain boundaries

T. A. Arias and J. D. Joannopoulos

Physics Department, Massachusetts Institute of Technology, Cambridge, Massachusetts 02139

(Received 3 September 1993)

We present the results of an extensive *ab initio* study of the $\Sigma=5$ tilt [310] grain boundary in germanium. We find that the boundary reliably reconstructs to the tetrahedrally bonded network observed in high-resolution electron microscopy experiments without the proliferation of false local minima observed in similar twist boundaries. The reduced density of bonds crossing the grain-boundary plane leads us to conjecture that the boundary may be a preferred fracture interface. Though there are no dangling bonds or miscoordinated sites in the reconstruction, the boundary presents electron-trap states just below the conduction band. Further, we show that lattice relaxation effects are irrelevant to the segregation of impurities to tetrahedrally reconstructed defects and that the interfacial electron-trap states give rise to an electronic frustration mechanism that selectively drives the segregation of only *n*-type dopants to the boundary.

I. INTRODUCTION

Already much progress has been made in completing the promise of quantum mechanics that it is at last possible to build a theory of our macroscopic world of real materials from the understanding of its basic constituents, electrons and nuclei. Since the introduction of density-functional theory, pseudopotential theory, and a series of ever more efficient computational schemes, the *ab initio* approach has yielded tremendous understanding of the thermodynamic properties of bulk materials,¹ crystal surface structures² and dynamics,³ the nature of point defects,⁴ and the diffusion and interaction of impurities in bulk.⁵ There remains one final important link in developing an *ab initio* understanding of the macroscopic world, an *ab initio* understanding of extended defects in crystals. Such defects are widely known to profoundly affect the properties of real materials such as electrical conductivity and ductility. To date, the *ab initio* study of such extended defects has been limited due to the high complexity of these systems (requiring large supercells) and the long length scales they involve (resulting in charge sloshing instabilities in the relaxation of the electronic system to the Born-Oppenheimer surface). However, Teter, Payne, and Allan⁶ and Gillan⁷ have recently introduced electronic relaxation schemes that make tractable the treatment of complex systems with large length scales and thus the *ab initio* exploration of this final frontier of extended defects.

Of the extended defects, grain boundaries are particularly important to understand from a practical point of view. Most modern electronic devices employ polycrystalline semiconductor materials, making the understanding of the electronic properties of these defects critical.⁸ Also, understanding the interaction of grain boundaries with dopants and impurities is important as many common dopants tend to segregate, collect, at the grain boundaries. This results in a complex interacting system affecting the conduction through the material. In fact, it is currently speculated that most of the electrical activity

of grain boundaries is not intrinsic but rather associated with the defects which tend to segregate at the grain boundaries.^{9,10}

Though much experimental progress has been made in the study of semiconducting grain boundaries in recent years [especially in the imaging of structures through high-resolution electron microscopy (HREM) (Ref. 11)], many important problems remain unsettled due to the inherent difficulties of the experimental isolation and study of phenomena deep in the bulk of materials. Such problems include understanding whether the distribution of interface states in the gap is due to the boundary or extrinsic defects, the specific mechanisms driving segregation of impurities to the boundary (especially of dopants), and the microscopic aspects of the interactions of grain boundaries with mechanical stress fields that eventually lead to fracture of the material.

In this paper we shall focus on developing a sufficient understanding of a particular instance of a grain boundary in an elemental semiconductor to permit insight into the above issues. This will entail understanding in detail the mechanical and electronic structure of the undoped grain boundary as well as its interactions with segregating species. For our material we choose germanium, whose polycrystalline forms are important in solar cell technology and whose well-known homology to silicon gives us confidence that our most general results will be relevant to experiments carried out in that material as well. For the boundary we take the $\Sigma=5$ tilt [310] boundary as a member of the large class of low-energy grain boundaries which preserve the local tetrahedral bonding network of the host crystal. We do this in the hope of fostering the generalization of our results to a large, relevant class of boundary. Such boundaries are especially relevant in cast polycrystalline materials, where we expect to see mostly low-energy symmetric grain boundaries.¹² Finally, for our dopants we will study arsenic for *n* type and gallium for *p* type.

This paper is organized as follows. We will begin in

Sec. II by briefly outlining the *ab initio* method we employ as well as the computational details germane to our grain-boundary calculations. Then, in Sec. III we will proceed to present our results on the structural and electronic properties of the undoped grain boundary, comparing and contrasting with experiment whenever possible. In Sec. IV we present results on the segregation of dopants to our grain boundary. Finally, in Sec. V we conclude the paper by showing how our results generalize, thus tying together the diverse experimental results on grain-boundary electrical conductivity and segregation.

II. *Ab initio* METHOD AND CALCULATIONAL DETAILS

The *ab initio* method employed for all of the calculations in this paper is the total energy density-functional approach. This means that an expression for the total energy of the system of electrons and ionic cores is minimized over all possible wave functions to yield the ground-state many-body charge density and energy of the system. In particular, to treat the electron-electron interactions, we use the standard Coulomb integral plus the Perdew-Zunger¹³ form for the local approximation to the exchange-correlation correction. For the electron-ion interactions we employ the pseudopotential approximation, using the local Starkloff-Joannopoulos potential for germanium and the dopant arsenic.¹⁴ The dopant gallium, however, requires use of a nonlocal pseudopotential and for this element we used the Kleinmann-Bylander form¹⁵ for the Hamman-Schluter-Chiang potential.¹⁶ Finally, the ion-ion interaction is a simple Madelung sum computed within the Ewald framework.

To perform these calculations, we use a supercell of atoms repeated periodically throughout all of space. We treat the Brillouin-zone integrations with a sum over three special k points¹⁷ in the irreducible zone that gives a denser coverage in reciprocal space than does using just the Γ point in a cubic supercell of 16 Å on a side. For our plane-wave basis, we have chosen a conservative cutoff of 200 eV, or 145 plane waves per ion. Previous work on the Ge(100) surface has shown that a cutoff of only ≈ 100 eV suffices to converge reconstruction energy differences on the order of 50 meV (similar to the energy differences that interest us) to an accuracy of better than 3 meV². This high accuracy is attained even with a modest cutoff because, as in our calculations, the energy differences of interest are between very similar systems. This means that in order to attain a modest precision in computing energy differences it is not necessary to first attain a high precision in the total energy of the system.

This general principle applies not only to convergence with plane-wave cutoff but also often to the cumulative effect of the various errors inherent in electron-structure calculations. As an illustration of this principle and to give an indication of the order of magnitude of the accuracy to which we may compute the energies of the subtle lattice distortions associated with dopant segregation, we have calculated the zone-center optic-phonon frequency in a two-atom germanium cell with the same cutoff and pseudopotential and with similar k -point sampling. The

results of this calculation agree with *experiment* to better than 3.3%. We then see that the aggregate effect of all of our approximations on computing the energies of lattice distortions typical in magnitude of those in our boundary system (≈ 50 meV) will be on the order of several meV.

Finally, we would like to comment on our choice of computational scheme for minimizing the electronic functional. We observed that as a result of the large length scales in our calculations (≈ 30 Å), the $1/G^2$ factor in the reciprocal lattice sums for the electronic Coulomb energy makes the response of the electronic system to long wavelength charge fluctuations so stiff that under a first-order equation of motion molecular-dynamics method¹⁸ for relaxing the electronic system, the electronic charge simply “sloshes” from end to end of our cell, without the system ever converging to its ground state. It is possible to attain convergence by reducing the effective length scale of our system by explicitly enforcing the screw-axis symmetry described below; however, attracted by the demonstrable freedom from this instability of the Teter, Payne, and Allan, and Gillan schemes and by those schemes’ greater efficiency for minimizing the electronic functional, we have chosen to employ the former conjugate-gradient technique over equation-of-motion methods for the bulk of the calculations presented below.

III. STRUCTURAL AND ELECTRONIC PROPERTIES OF THE UNDOPED BOUNDARY

To study $\Sigma=5$ tilt [310] boundary, we employ a supercell of 68 atoms containing two slabs of bulk material whose interfaces, after relaxation, form the two grain boundaries of our cell. (Because the supercell is repeated periodically, our cell by necessity contains two boundaries.) To produce the desired boundary, the initial slabs or “grains” are oriented with a relative rotation of $\cos^{-1} 0.6$ about the [001] axis so that their $[\bar{1}30]$ and $[1\bar{3}0]$ axes coincide. The two boundary interfaces are then parallel to the (310) plane of either bulk slab, and each cut through one shared plane of atoms. The periodicity of the interface requires our supercell to be at least one conventional cubic unit cell in height (5.65 Å) along the [001] direction and to extend 8.94 Å in the $[\bar{1}30]$ direction. We choose this minimal reconstructive unit cell in the boundary plane and extend our cell 34 planes of atoms (30.4 Å) perpendicular to the boundary, in the [310] direction. With the grain orientation and the boundary plane defined, the only remaining degree of freedom in specifying the boundary geometry is the relative translation of the grains. This may be determined either by α -fringe measurements¹⁹ which give a relative grain displacement of $\approx \frac{1}{8}[001] + 0.0075[310]$ with a “negligible” shift along the $[\bar{1}30]$ direction or by direct imaging through HREM, which gives essentially the same results.¹¹ We choose to use a displacement of $\frac{1}{8}[001]$, which as observed by Bacmann *et al.*¹⁹ is most compatible with the symmetry of the boundary, and opt to ignore the barely measurable 0.02-Å expansion of the boundary.²⁰ This completes the specification of the *ini-*

tial locations of the ions in our calculation except for those lying on the two interface planes and shared by the two grains, which we simply place at the mean location required by the two grains. Finally, because our two boundaries by necessity have opposite orientation, we may impose, without loss of generality, a screw-axis symmetry of rotation π and displacement of half the length of our cell along the $[310]$ direction. In this initial arrangement there is a lack of tetrahedral order and much corresponding internal strain with many bonds formed far from the preferred sp^3 tetrahedral angles and the presence of both threefold rings and atoms with reduced coordination (See Fig. 1).

With the initial atomic positions described above, we then solve for the electronic wave functions as described in Sec. II, determine the resulting forces on the atoms from the Hellmann-Feynman theorem, and move the boundary atoms and all other atoms up to and including their third-nearest neighbors along these forces, maintaining the symmetry axis described above, until the maximum force on any atom in the system is less than 0.09 eV/\AA in each direction.²¹ This procedure keeps four layers of atoms in each grain fixed at their "ideal" bulk locations. Despite the highly defected nature of the initial configuration, under this simple procedure the system immediately relaxes to the experimentally observed structure, strongly indicating that this tilt boundary has one well-defined global minimum rather than several closely related local minima, as observed in group-IV *twist* boundaries.²² Comparing the projection of our predicted atomic locations into the (001) and $(\bar{1}\bar{3}0)$ planes with HREM results from thin films oriented along the same directions gives experimental verification of our *ab initio* prediction of the boundary reconstruction.¹¹ (See Fig. 2.) This unique opportunity to compare directly the full three-dimensional experimental structure of an internal material interface with the reconstruction we can calculate with *no adjustable parameters* illustrates the accuracy and predictive power of state-of-the-art *ab initio* techniques.

The structure we determine both confirms the structure insightfully proposed by Bacmann *et al.*¹⁹ only on the basis of the α -fringe grain displacements and rein-

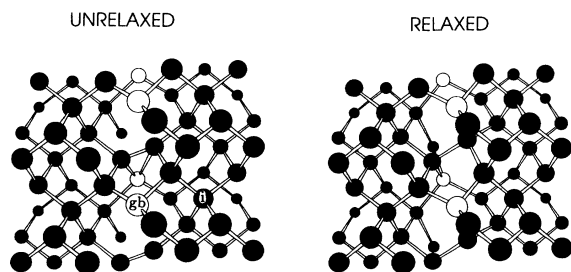


FIG. 1. Three-dimensional perspective drawing of the atomic locations about the boundary plane before and after relaxation. Gray and black circles represent atoms of each grain, respectively, while the white circles represent the boundary atoms initially located on the geometric boundary and shared by both grains. The atoms labeled *gb* and *i* refer to substitutional sites for dopants. (See text.)

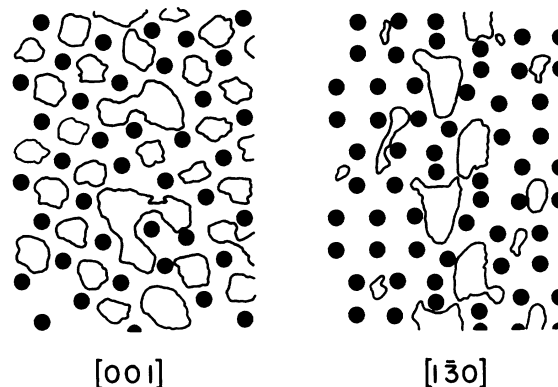


FIG. 2. Comparison of the calculated locations of atom columns (solid circles) and HREM transmission of electrons (outlined areas) along both the $[001]$ and the $[\bar{1}\bar{3}0]$ directions. In both panels the $[310]$ direction runs horizontally from left to right and the projection of the boundary plane runs from top to bottom. The HREM transmission regions are after Refs. 11 and 27.

forces the atomic positions and energies calculated by other authors with semiempirical approaches for the same boundary in the homologous silicon system. Our coordinates, for example, correspond very closely (to within a hundredth of a lattice constant) to the positions quoted by Paxton and Sutton for silicon.²³ Furthermore, we calculate a rather low interfacial energy of 260 erg/cm^2 , in line with the 300 erg/cm^2 quoted in Ref. 23 and the 260 erg/cm^2 computed in Ref. 24 for the silicon system.

In this reconstruction the crystal has completely restored its tetrahedral bonding network (see Fig. 1) with all bond lengths and bond angles within 3.3% and 19° , respectively, of the bulk values. This tetrahedral reconstruction not only leads to a low interface energy but also lends stability to this reconstruction in terms of the aforementioned lack of several low-energy local minima. Such low-energy tetrahedral reconstructions are often formed in tilt boundaries because of their ability to reconstruct as a linear array of simple structural units.^{25,26} In contrast, twist boundaries cannot be built from such simple arrays of linear units, do not tend to form tetrahedral reconstructions, and, consequently, are much higher energy defects (by factors of 4) and often exhibit many low-lying false local minima.²² Though the tetrahedral bonding is preserved in our boundary, there are subtle topological differences from the bulk when we get out to fifth-nearest neighbors, as our reconstruction has both 5- and 7-member rings in addition to the sixfold rings of which the bulk consists entirely. As we shall see below, these subtle topological differences will interact most strongly with excitations that remain coherent over extended length scales, such as electrons, rather than with incoherent excitations, such as the lattice relaxation around an impurity. Finally, in this structure there is a 50% reduction in the number of bonds crossing the boundary plane from the number that connect (310) planes in the bulk (from six per 50.6 \AA^2 cell to four), so that fracture of the crystal along this interface will create

a correspondingly lower density of dangling bonds, suggesting that this boundary is a preferred interface for fracture.

Because of our use of an *ab initio* technique, we simultaneously gain highly reliable information on both the atomic positions and the electronic states of the boundary. The distribution of the electronic states of our 68-atom cell near the bulk gap shows that there are no boundary states for holes derivative of the valence band but points to the presence of an interface band for electrons on the order of 10 meV below the conduction band (Fig. 3). Examination of the projection of charge density of the lowest empty band in our cell along the [310] axis confirms the localization of these states on the boundary (Fig. 4). The existence of these localized states is made possible in the absence of dangling bonds by the interaction of the extended nature of electronic wave functions with the subtle topological differences seen in the grain-boundary reconstruction. Though the experimental situation is unclear due to the influences of segregating species and the tendency of even our simple boundary to form "coherent" steps,²⁷ current-voltage characterizations of bicrystal²⁸ and polycrystalline samples²⁹ have consistently shown that grain boundaries in germanium, though providing effective traps for electrons, do not trap holes, as has been observed by other authors.⁹ Though our results complement this picture, it should be stressed that the electron-trap states in germanium are observed by various experimental techniques to be much deeper in the gap than we have calculated, almost reaching the top of the valence band.^{30,31} The depth of the states in the experiments is most likely related to the presence of defects in the boundary reconstructions (such as steps) and not related to the intrinsic structure of the reconstructed tilt boundaries. As we shall see, the primary consequence of our idealized boundary having much shallower electron-trap states only will be to modify the quantita-

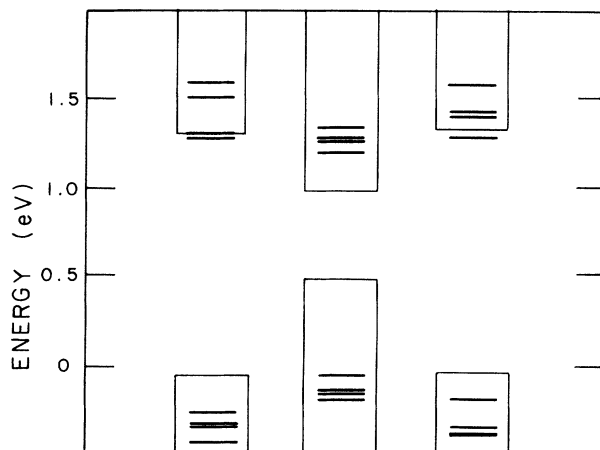


FIG. 3. The eigenenergies of the states for the relaxed grain boundary in our supercell at the three k points in our Brillouin-zone sampling scheme (horizontal lines) and the corresponding interface-projected bulk states (rectangular boxes). Note the presence of shallow gap states near the top of the gap at the k points on the left and right.

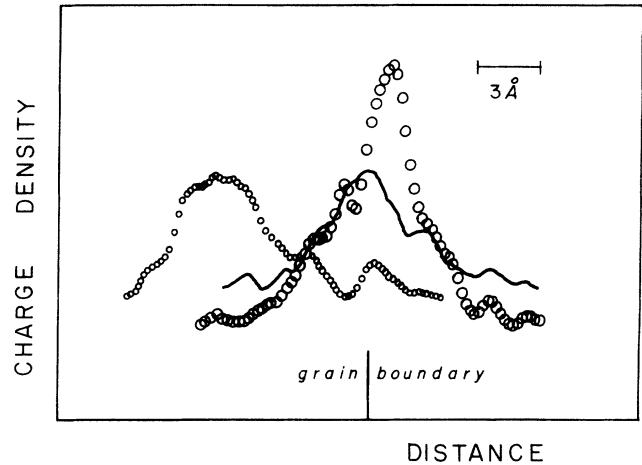


FIG. 4. Charge density of the lowest empty band in the undoped boundary (solid curve) and of the donor electron for a dopant arsenic on the boundary (large circles) and far from the boundary (small circles) projected along the [310] axis. Note that when the dopant is far from the boundary, both it and the boundary compete for the donated electron, whereas when the dopant is placed directly on the boundary, the competition is relieved and the charge strongly localizes on the boundary. See text for discussion.

tive but not the qualitative picture we build from studying this one boundary.

IV. SEGREGATION

To study segregation at the $\Sigma=5$ tilt [310] boundary, we have substituted both gallium and arsenic in three different locations; (1) the center of our fixed bulk layers, (2) the intermediate site i , and (3) the boundary in site gb . (See Fig. 1.) To maintain the screw-axis of our cell, the two boundaries in our cell are doped symmetrically. With the impurities at these locations, we first calculate the energy of the system with the lattice held fixed and then relax the dopants and all surrounding atoms, again, out to third-nearest neighbors. Despite the bulklike reconstruction of the boundary, without defects like dangling bonds or sub- or extracoordinated sites, we still find a significant (0.1 eV) tendency for arsenic to segregate to the boundary. (See Fig. 5, left.) This behavior is representative of the experimentally observed tendency of arsenic to exhibit equilibrium segregation to grain boundaries in samples of doped polycrystalline semiconductors.³²

The device of first holding the host lattice frozen in the presence of an impurity and later permitting relaxation separates lattice relaxation from electronic effects and fosters insight into the mechanisms driving segregation. The relaxation energy we observe as the lattice responds to the impurity measures the elastic energy associated with incorporation of the impurity into the lattice. Notice that although the relaxation energy is a significant energy (nearly one-half of the final binding to the boundary), the differences in the elastic incorporation energy as the impurity move from site to site are much smaller than

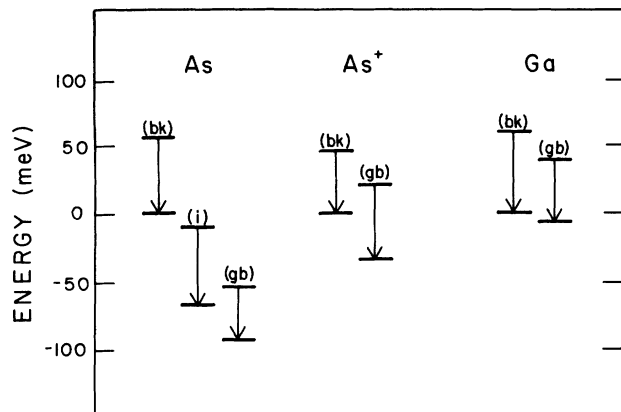


FIG. 5. Energy-level diagram for doping the boundary with arsenic (As), an ionized arsenic donor (As^+), and gallium (Ga) with the dopant placed in the center of the bulk slabs (bk), at the intermediate location (i), and directly on the grain boundary (gb). The horizontal lines represent the energy of the system with the surrounding lattice held fixed (arrow tails) and with the surrounding lattice allowed to relax up to third-nearest neighbors (arrow heads). All energies are measured relative to the fully relaxed energy of the respective dopant in bulk.

the final binding to the boundary (Fig. 5, left). This is in agreement with our expectation that incoherent excitation effects like elastic expansions do not depend on subtle topological features of the lattice and are not affected strongly by the presence of the boundary. This weak interaction of the boundary lattice with the impurity strongly suggests that the mechanism for segregation is electronic, as opposed to mechanical, in nature.

The boundary conduction states observed in Sec. III provide the electronic mechanism for the segregation. There is a natural frustration in the dopant-boundary system as both the As^+ ion and the low-energy interface states compete for the donor electron. This frustration, however, is simply relieved by placing the impurity on the boundary. (See Fig. 4.) Note that when the impurity is far from the boundary, the donor electron prefers to stay with the dopant, demonstrating that the surface band must lie between the conduction band and the hydrogenic state of an isolated arsenic germanium, some 13 meV below the conduction band, consistent with our band-structure results. To demonstrate that frustration caused by the donor electron is indeed responsible for the binding to the boundary, we have removed the donor electron from the highest band (which we identify from Fig. 4 as the As donor state) and then studied the segregation of As^+ .³³ As expected, the interaction with the boundary is dramatically reduced (by a factor of 3; Fig. 5, center) down to room temperature. Further, comparing the energies of the neutral systems and ionized systems (with the ions held fixed during the ionization process), we find that the ionization potential of the As is increased by roughly 80 meV by virtue of its proximity to the boundary. This accounts for most of the binding to the boundary. Also, with the ionization energy so increased, the arsenic dopants near the boundary retain their electrons and thus lose their electrical activity, as is ob-

served experimentally for arsenic,³² and continue to experience the frustration-induced attraction even at elevated temperatures.

Next, we turn to the segregation of a p -type dopant, gallium. (See Fig. 5, right.) As expected, lattice relaxation around the impurity is a significant energy but remains insensitive to the location of the dopant and thus cannot contribute significantly to the interaction with the boundary. Moreover, because of the lack of boundary hole states as observed in Sec. III, there is now no competition for the donated carrier, no resulting frustration effect, and very little net interaction with the boundary. Though the experimental results on dopant segregation are enigmatic, it has been observed that when care is taken to ensure an equilibrium distribution, arsenic and phosphorous segregate to elemental semiconductor grain boundaries, whereas boron does not.^{32,34} Our calculations again complement the qualitative results of experimental studies and now suggest a general picture: n -type but not p -type dopants segregate in germanium. Quantitatively, the experimentally determined binding energies are significantly larger (~ 0.5 eV) than what we have calculated; however, this is attributable to the presence of deep extrinsic electron-trap states (broken bond defects, dislocations, etc.) naturally occurring in the experimental boundary, which would result in larger dopant-binding energies.

V. GENERALIZATIONS AND PREDICTIONS

Though we have studied just one particular grain boundary, the behavior of our boundary is representative in many aspects of the behavior of the ensemble of boundaries found in polycrystalline samples, and our study suggests the following general picture.

Tetrahedrally rebonded grain boundaries not only are low in energy, they also reconstruct reliably without falling into false local minima. Further, tetrahedrally reconstructed boundaries respond to incoherent excitations, such as elastic effects around an impurity, very much in the same way as does the bulk, so that these excitations are relatively blind to the presence of the boundary. More coherent excitations such as electrons, on the other hand, sense the subtle topological differences (e.g., fivefold and sevenfold rings) between the bulk and boundary and may bind to the boundary in bona fide interface states, even in boundaries without dangling bonds.

In our picture, these general features then have important implications regarding the ability of these rebonded boundaries to bind dopants. Mechanical effects in the incorporation of the impurity do not contribute significantly to the impurity-boundary interaction, leaving electronic phenomena alone to drive segregation. Without dangling bonds, the one electronic feature which may distinguish the boundary from the bulk is the presence of localized states which may compete for the carrier donated by the impurity. This not only explains the result that the boundary we studied binds arsenic but not As^+ or gallium, it also predicts that this boundary will bind n -type but not p -type dopants. Further, if we were to divide all of the tetrahedrally reconstructed grain

boundaries into classes based on segregation behavior, we should find just four simple classes: those boundaries which attract either n -type but not p -type impurities, p -type but not n -type impurities, both groups, or neither, depending on whether the particular boundary localizes either electrons but not holes, holes but not electrons, both types of carrier, or neither, respectively. We saw that this expectation is borne out in germanium, where the boundaries, almost without exception, both trap electrons, but not holes and attract n -type but not p -type impurities. Although the presence of imperfect reconstructions with dangling bonds is indicated in the experimental boundaries by the experimental trap states being so deep into the gap and the dopant-boundary energies being so large, the basic reasoning behind the electronic-frustration effect remains intact and we should still ex-

pect the observed correlation between carrier trapping and segregation.

Finally, our arguments about tetrahedrally coordinated grain boundaries make no reference to the dimensionality of the defect, so that dislocations or local defects that find tetrahedral rebondings should also exhibit the same behaviors. They also may have localized electron or hole states and so attract n -type or p -type dopants through the same mechanisms we have identified.

ACKNOWLEDGMENTS

This work was supported in part by U.S. AFOSR Contract No. 87-0098. T.A.A. acknowledges support from AT&T Bell Laboratories. The authors thank M. Kohyama for helpful discussions.

¹F. Buda, R. Car, and M. Parrinello, Phys. Rev. B **41**, 1680 (1990).

²M. Needels, M. C. Payne, and J. D. Joannopoulos, Phys. Rev. B **38**, 5543 (1988).

³S. Ihara, S. L. Ho, T. Uda, and M. Hirao, Phys. Rev. Lett. **65**, 1909 (1990).

⁴M. Needels, J. D. Joannopoulos, Y. Bar-Yam, and S. T. Pantelides, Phys. Rev. B **43**, 4208 (1991).

⁵C. G. Van de Walle, Y. Bar-Yam, and S. T. Pantelides, Phys. Rev. Lett. **60**, 2761 (1988).

⁶M. Teter, M. Payne, and D. Allan, Phys. Rev. B **40**, 12 255 (1989).

⁷M. J. Gillan, J. Phys. Condens. Matter. **1**, 689 (1989).

⁸C. Y. Wong, C. R. M. Grovener, P. E. Batson, and D. A. Smith, J. Appl. Phys. **57**, 2 (1985).

⁹C. R. M. Grovener, J. Phys. C **18**, 4079 (1985).

¹⁰K. Masuda-Jindo and Y. Fujita, in *Polycrystalline Semiconductors II*, edited by J. H. Werner and H. P. Strunk, Springer Proceedings in Physics Vol. 54 (Springer, Berlin, 1992), p. 139.

¹¹A. Bourret, J. L. Rouviere, and J. M. Penisson, Acta Crystallogr. Sec. A **44**, 838 (1988).

¹²F. Kominou, T. Karakostas, and G. L. Bleris, J. Phys. Colloq. **43**, Cl-9 (1982).

¹³P. Perdew and A. Zunger, Phys. Rev. B **23**, 5048 (1981).

¹⁴Th. Starkloff and J. D. Joannopoulos, Phys. Rev. B **16**, 5212 (1977). For germanium we used the parameters $\lambda_c = 18$ and $r_c = 1.05$ a.u., which reproduce the atomic wave functions and eigenvalues to within 2%. For arsenic we use the parameters $\lambda_c = 10.196$ and $r_c = 0.973$ giving results of similar quality.

¹⁵L. Kleinmann and D. M. Bylander, Phys. Rev. Lett. **4**, 1425 (1982).

¹⁶D. R. Hamann, M. Schluter, and C. Chiang, Phys. Rev. Lett. **43**, 1494 (1979).

¹⁷H. J. Monkhorst and J. D. Pack, Phys. Rev. B **13**, 5188 (1976).

¹⁸M. C. Payne, J. D. Joannopoulos, D. C. Allan, M. P. Teter, and D. H. Vanderbilt, Phys. Rev. Lett. **56**, 2625 (1986).

¹⁹J. J. Bacmann, A. M. Papan, M. Petit, and G. Silvestre, Philos. Mag. A **51**, 697 (1985).

²⁰Distributed over the 13 planes about each boundary which are

allowed to relax, this amounts to an error in atomic position of less than 0.0016 \AA , or an elastic energy on the order of less than 1 meV per grain, on a simple ball and spring model with the spring constant from the Γ phonon mode, 23 eV/\AA^2 .

²¹Using the same simple spring model of Ref. 20 and the residual forces on our ions, we estimate the residual ionic relaxation error to be on the order 2 meV per interface. The residual relaxation errors for all of our ionic relaxations are typically at this level.

²²E. Tarnow, P. Dallot, P. D. Bristowe, and J. D. Joannopoulos, Phys. Rev. B **42**, 3644 (1990).

²³A. T. Paxton and A. P. Sutton, J. Phys. C **21**, L481 (1988).

²⁴M. Kohyama, R. Yamamoto, Y. Ebata, and M. Kinoshita, J. Phys. C **21**, 3205 (1988).

²⁵A. P. Sutton and V. Vitek, Philos. Trans. R. Soc. London, Ser. A **309**, 1 (1983).

²⁶A. P. Sutton, Int. Metall. Rev. **29**, 377 (1984).

²⁷A. Bourret and J. L. Rouviere, in *Polycrystalline Semiconductors, Grain Boundaries and Interfaces*, edited by H. Möller et al., Springer Proceedings in Physics Vol. 35 (Springer, Berlin, 1988), p. 8.

²⁸W. E. Taylor, N. H. Odell, and H. Y. Fan, Phys. Rev. **88**, 867 (1952).

²⁹H. F. Mataré, J. Appl. Phys. **56**, 2605 (1984).

³⁰A. Broniatowski and J. C. Bourgoin, in *Grain Boundaries in Semiconductors*, edited by H. J. Leamy, G. E. Pike, and C. H. Seager (North-Holland, New York, 1982), p. 119.

³¹N. Tabet, C. Monty, and Y. Marfaing, in *Polycrystalline Semiconductors, Grain Boundaries and Interfaces* (Ref. 27), p. 89.

³²J.-L. Maurice, in *Polycrystalline Semiconductors II* (Ref. 10), p. 166.

³³To avoid dealing with a periodic system containing a net charge, we introduce into the As^+ calculations a neutralizing charge background, whose effect we must estimate in order to calculate the *total energy* of the system [See E. Tarnow, S. B. Zhang, K. J. Chang, and D. J. Chadi, Phys. Rev. B **42**, 11 252 (1990).] However, by considering only appropriate *energy differences*, as we have done in the present work, one can arrange that the correction terms associated with the neutralizing background, which are nearly independent of the position of the charged defect, cancel. Using this procedure, for ex-

ample, Y. Bar-Yam and J. D. Joannopoulos, *Phys. Rev. B* **30**, 2216 (1984) obtained periodic supercell results on energy differences in the migration of charged self-interstitials in silicon which agree to better than 20% with the aperiodic Green's function results of R. Car, P. J. Kelly, A. Oshiyama, and S. T. Pantelides, *Phys. Rev. Lett.* **52**, 1814 (1984).

³⁴Although we do have direct experimental information for the segregation of boron (see Ref. 32), we have yet to perform calculations with it as a dopant because the much higher cutoff energy associated with the accurate description of this first-row element would make the computation prohibitive.